Nonlinear Dyn
https://doi.org/10.1007/s11071-020-05746-9

ORIGINAL PAPER

Precursor criteria for noise-induced critical transitions in multi-stable systems

Jinzhong Ma · Yong Xu · Yongge Li · Ruilan Tian · Guanrong Chen · Jürgen Kurths

Received: 12 August 2019 / Accepted: 4 June 2020

Abstract Predicting noise-induced critical transitions between multi-stable states of a dynamical system is of uttermost importance in various fields. This paper investigates a tri-stable model with desirable, sub-desirable and undesirable states as a prototype class of real systems. Then, two critical transitions, from the desirable state to the sub-desirable one (CT1) and from the sub-desirable state to the undesirable one (CT2), induced by Gaussian white noise are uncovered. The new results show that the noise-induced CT1 and CT2 take place before the bifurcation point of the corresponding deterministic system and this phenomenon becomes earlier with increasing noise intensity. Therefore, some precursor criteria of the noise-induced CT1 and CT2 are further explored. Firstly, the largest Lyapunov exponent and the Shannon entropy are introduced into the prediction of the noise-induced CT1 and CT2 from a new perspective. It is found that both of them are more efficient compared to the classic variance and auto-correlation at-lag-1, and the Shannon entropy is more robust as compared to CT1 and CT2 under strong fluctuations. Moreover, a range of the bifurcation parameter, where noise-induced critical transitions may occur, is approximately quantified in the parameter-dependent basin of the unsafe regime. All of these results may provide some guidance for establishing

J. Ma · Y. Xu
Department of Applied Mathematics, Northwestern Polytechnical University, Xi'an 710072, China

Y. Xu (✉)
MIIT Key Laboratory of Dynamics and Control of Complex Systems, Northwestern Polytechnical University, Xi'an 710072, China
e-mail: hsux3@nwpu.edu.cn

Y. Li
Center for Mathematical Sciences and School of Mathematics and Statistics, Huazhong University of Science and Technology, Wuhan 430074, China

R. Tian
Department of Engineering Mechanics, Shijiazhuang Tiedao University, Shijiazhuang 050043, China

G. Chen
Department of Electrical Engineering, City University of Hong Kong, Hong Kong 999077, China

J. Kurths
Potsdam Institute for Climate Impact Research, 14412 Potsdam, Germany

J. Kurths
Department of Physics, Humboldt University at Berlin, 12489 Berlin, Germany

Published online: 18 June 2020

more general precursor criteria of multiple noise-induced critical transitions in the future.

Keywords Tri-stable model · Gaussian white noise · Critical transition · Largest Lyapunov exponent · Shannon entropy · Parameter-dependent basin of the unsafe regime

1 Introduction

It is an ubiquitous phenomenon that many practical systems undergo multi-stable states with gradually changing conditions [1, 2]. Typical examples include metabolic systems [3], protein folding [4], chemical reactions [5], endogenous molecular-cellular networks [6] and thermohaline ocean circulation [7]. Nowadays, critical transitions between multi-stable states have become a major focus in many research fields, where every transition from one stable state to another one could cause serious problems such as significant losses that may affect human wellbeing [8–11].

To avert such catastrophic transitions, numerous studies have been carried out, suggesting that the use of generic early warning indicators can detect the proximity of a system to a critical transition [12, 13]. Two of the most widely used indicators are increasing variance [14] and autocorrelation [15]; both were established through a critical slowing down [16]. Other indicators include skewness [17], flickering [18] and spatial correlation [19]. While a large body of work has been devoted to the study of systems exhibiting only one critical transition, much less is known about the dynamics of systems undergoing a multitude of stable states.

In systems with multi-stable states, gradually changing conditions may have a little effect on the current stable state, but may nevertheless reduce the height of the potential barrier in terms of stability landscapes [20]. This loss of resilience makes the system more fragile in the sense that it can easily be tipped into different states by stochastic fluctuations. If these fluctuations are strong, a critical transition may take place earlier. Therefore, precursors that simultaneously warn multiple earlier critical transitions are important, so they need to be further explored.

In fact, the occurrence of noise-induced critical transitions is closely related to the system's stability. When a system approaches a critical point, stochastic fluctuations can easily cause a loss of stability and then drive the system to shift to a different stable state [21–23]. As is well known, the largest Lyapunov exponent and the Shannon entropy are two appropriate measures to quantify the instability in dynamical systems [24–26]. Hence, in this paper, both of them are introduced into the prediction of the noise-induced CT1 and CT2 from a new perspective. Furthermore, a range of the bifurcation parameter, where noise-induced critical transitions may occur, will be approximately quantified in terms of basin stability [27, 28]. This will be another precursor, called the parameter-dependent basin of the unsafe regime (PDBUR) [29].

This paper is organized as follows: Sect. 2 analyzes the noise-induced CT1 and CT2 in a given tri-stable system. The effectiveness of the largest Lyapunov exponent and the Shannon entropy for early warnings of CT1 and CT2 is investigated in Sects. 3 and 4, respectively. Section 5 approximately quantifies the range of the bifurcation parameter, where the two noise-induced critical transitions may occur. Finally, this paper is concluded with Sect. 6.

2 Two noise-induced critical transitions in a tri-stable system

Undergoing different states is a common phenomenon in various real-world systems. For example, human cells may undergo healthy, sub-healthy and cancer states [30]. If a body stays in a sub-healthy state, namely the early stage of the disease, it still has a long time for the whole organism being viable. Now, the intervention of treatment may recover the body to the healthy state. However, the best time for a treatment is missed if the body shifts to the cancer state and it is difficult to return to the sub-healthy state even if the body is treated.

To warn these catastrophic transitions, some precursors will be explored via a self-constructed tri-stable model containing desirable, sub-desirable and undesirable states. The form is

$$dx = f(x,\alpha)dt + \sqrt{\sigma}dB(t), \tag{1}$$

where $f(x,\alpha) = -\frac{\partial U(x,\alpha)}{\partial x}$ and $U(x,\alpha) = \frac{19}{100}x^6 + \frac{2}{25}x^5 - \frac{23}{20}x^4 - \frac{1}{6}x^3 + \frac{19}{10}x^2 + \alpha x$, $U(x,\alpha)$ represents the potential function, α is a bifurcation parameter, $B(t)$ is a Brownian motion and σ denotes the noise

intensity. These special coefficient values are chosen to construct a simple model that roughly fits practical systems.

Figure 1 shows the equilibrium point x_E satisfying $\frac{\partial U(x_E,\alpha)}{\partial x} = 0$. The branches where x_{S1}, x_{S2} and x_{S3} are located represent the desirable state, sub-desirable state and undesirable state, respectively. Moreover, the branches where x_{U1} and x_{U2} are located mark the border between two stable branches. The coordinate values of the four bifurcation points, Fold1, Fold2, Fold3 and Fold4, are $(\alpha_{\text{Fold1}} = 0.65, x_{E-\text{Fold1}} = 1.343)$,$(\alpha_{\text{Fold2}} = -1.26, x_{E-\text{Fold2}} = 0.537)$, $(\alpha_{\text{Fold3}} = 1.50, x_{E-\text{Fold3}} = -0.586)$ and $(\alpha_{\text{Fold4}} = -2.15, x_{E-\text{Fold3}} = -1.576)$, respectively. If x_E approaches Fold1 or Fold3, a slight incremental change in α may cause a critical transition from the desirable state to the sub-desirable state (CT1) or a transition from the sub-desirable state to the undesirable state (CT2). Although there may be another critical transition from the desirable state to the undesirable one in the range of $\alpha \in [\alpha_{\text{Fold4}}, \alpha_{\text{Fold2}})$, the probability is small unless there are some discontinuous large jumps [31, 32]. Therefore, only the effects of Gaussian white noise on CT1 and CT2 are investigated below.

Figure 2 shows the effect of Gaussian white noise on two critical transitions. It can be seen that noise-induced CT1 and CT2 approaches Fold1 and Fold3, respectively, when σ is small, while both of them take place much earlier with increasing σ. For example, CT1 occurs at $\alpha = 0.3 < \alpha_{\text{Fold1}}$ for $\sigma = 0.1$ or $\sigma = 0.5$, and CT2 occurs at $\alpha = 0.9 < \alpha_{\text{Fold3}}$ for $\sigma = 0.5$. In addition, the interval between CT1 and CT2 becomes smaller with a further increase in σ. Therefore, it needs to explore the precursors that are sensitive to noise-induced critical transitions in multi-stable systems.

To further explain the phenomenon that the critical transitions take place earlier due to noise, the stationary probability density function (SPDF) of system (1) is theoretically analyzed in the following [33]. System (1) can be understood in the increment sense, as

$$\Delta x = f(x,\alpha)\Delta t + \sqrt{\sigma}\Delta B(t).$$

Using this equation, one can evaluate the coefficients of the Fokker–Planck–Kolmogorov (FPK) equation for the solution process x, as shown below, with

$$A(x,t) = \lim_{\Delta t\to 0}\frac{1}{\Delta t}E[\Delta x] = f(x,\alpha),$$

$$D(x,t) = \lim_{\Delta t\to 0}\frac{1}{\Delta t}E\left[(\Delta x)^2\right] = \sigma.$$

The forward FPK equation reads

$$\begin{aligned}\frac{\partial p(x,t)}{\partial t} &= -\frac{\partial}{\partial x}[A(x,t)p(x,t)] + \frac{\partial^2}{\partial x^2}\left[\frac{D(x,t)}{2!}p(x,t)\right] \\ &= -\frac{\partial}{\partial x}[f(x,\alpha)p(x,t)] + \frac{\sigma}{2}\frac{\partial^2 p(x,t)}{\partial x^2}\end{aligned} \tag{2}$$

where $p(x,t)$ denotes a probability density function

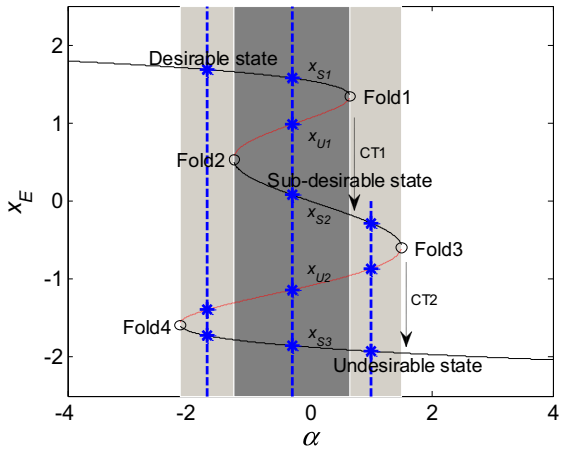

Fig. 1 Equilibrium states of system (1) with respect to $\sigma = 0$ and the changing α

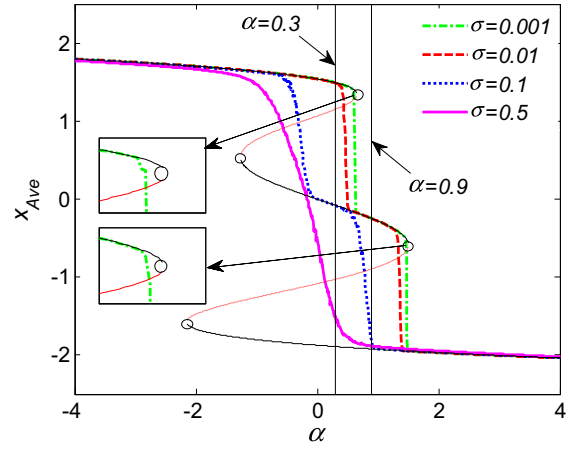

Fig. 2 Noise-induced CT1 and CT2 of system (1) for different σ. x_{Ave} denotes the average state of x in the presence of noise. Inset plots show that the critical points approach Fold1 and Fold3, respectively

(PDF) of x. Note that Eq. (2) can also be written in the form of

$$\frac{\partial p(x,t)}{\partial t}+\frac{\partial J(x,t)}{\partial x}=0,$$

where

$$J(x,t)=f(x,\alpha)p(x,t)-\frac{\sigma}{2}\frac{\partial p(x,t)}{\partial x},$$

and it has to be interpreted as a probability current. For a stationary process, $J(x,t)$ must be constant. So, one has

$$\frac{\partial p(x,t)}{\partial t}=0.$$

Hence, the PDF is independent of time. Suppose the process takes place on an interval $x\in[a,b]$, and the probability of being on the boundary $x=a$ or $x=b$ is zero. Then,

$$J(x,t)=0.$$

Therefore, the stationary solution satisfies

$$f(x,\alpha)p_s(x)-\frac{\sigma}{2}\frac{\partial p_s(x)}{\partial x}=0, \tag{3}$$

where $p_s(x)$ is the SPDF. Solving Eq. (3), we get

$$\begin{aligned}p_s(x)&=\frac{N}{\sigma}\exp\left[\frac{2}{\sigma}\int_a^x f(x',\alpha)\mathrm{d}x'\right]\\&=N\exp\left[-ln\sigma-\frac{2}{\sigma}\int_a^x\Big(-1.14x'^5-0.4x'^4\right.\\&\quad\left.+4.6x'^3+0.5x'^2-3.8x'-\alpha\Big)\mathrm{d}x'\right],\end{aligned} \tag{4}$$

where N is a normalization constant such that

$$\int_a^b p_s(x)\mathrm{d}x=1.$$

Based on Eq. (4), the SPDFs for a fixed α and four different σ are shown in Fig. 3. It can be seen that system (1) always stays in the desirable state when $\sigma=0.001$ and $\sigma=0.01$. However, the $p_s(x)$ in the desirable state is 0 for larger noise, here $\sigma=0.1$, and its peak appears in the sub-desirable state, which means that the earlier noise-induced CT1 occurs for $\alpha=0.3$. With a further increase in σ, $p_s(x)$ changes from one peak to two, and the two peaks appear in the sub-desirable state and undesired state, respectively. Since the peak in the sub-desirable state is much higher than that in the undesired one, CT2 will take place earlier for this α. These phenomena in $p_s(x)$ are consistent with the results of $\alpha=0.3$ shown in Fig. 2, which uncover the earlier critical transitions under noise.

3 Largest Lyapunov exponent

In stochastic dynamics, the largest Lyapunov exponent, labeled λ, is a useful method to detect the qualitative changes of the system with changing control parameters [25, 34, 35]. Here, it is introduced into the prediction of the noise-induced CT1 and CT2 from a new perspective, and Benettin's method is used to calculate it [36, 37].

Figure 4 shows the λ of system (1) for different values of σ. It is found that there is an obvious increase for λ before the noise-induced CT1 or CT2 when $\sigma=0.001$ or $\sigma=0.01$, which indicates that λ can act as an efficient precursor of CT1 and CT2 under small fluctuations. Although the increase in λ before CT2 becomes not so obvious when $\sigma=0.1$, the earlier CT1 and CT2 can still be identified by λ. As σ increases to 0.5, the spacing between CT1 and CT2 reduces. Only an increase for λ can warn the impending noise-induced critical transitions, while it cannot specify which one of CT1 and CT2 will occur. However, it can provide some useful signals for us to take some management in advance.

In a space diagram of λ as shown in Fig. 5, the earlier increase in it with increasing σ reflects its sensitivity to the earlier noise-induced CT1 and CT2. However, the change of λ from two peaks to one indicates that it is not accurate to CT1 and CT2 under larger σ.

All these results show that λ can be acted as an efficient precursor of noise-induced critical transitions in multi-stable systems with small fluctuations, but it cannot accurately illustrate which one of the multiple critical transitions occurs under strong fluctuations.

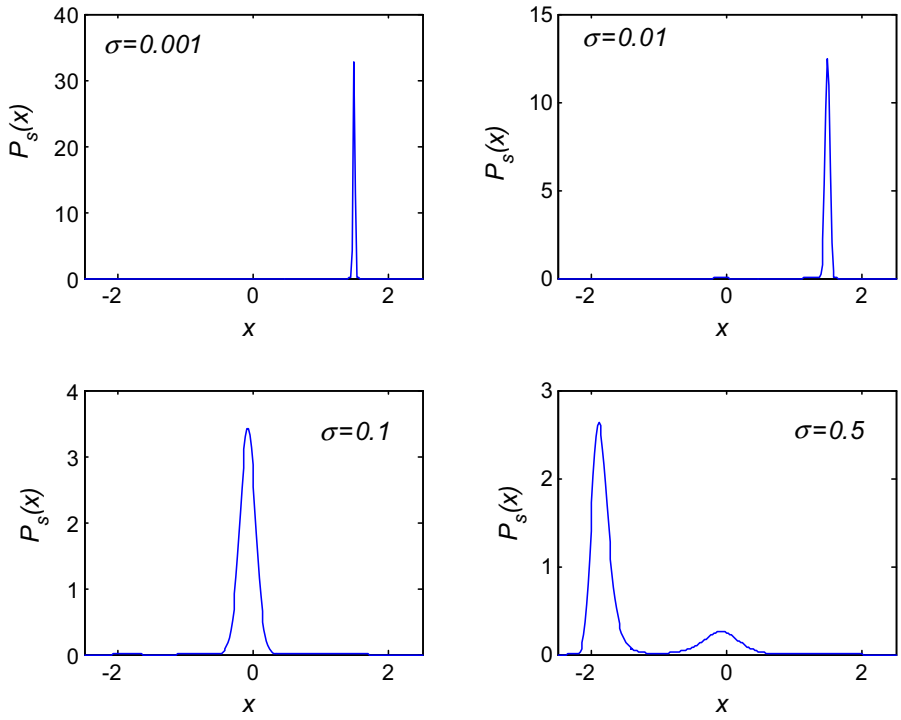

Fig. 3 SPDFs of Eq. (4) for $\alpha = 0.3$ and four different σ

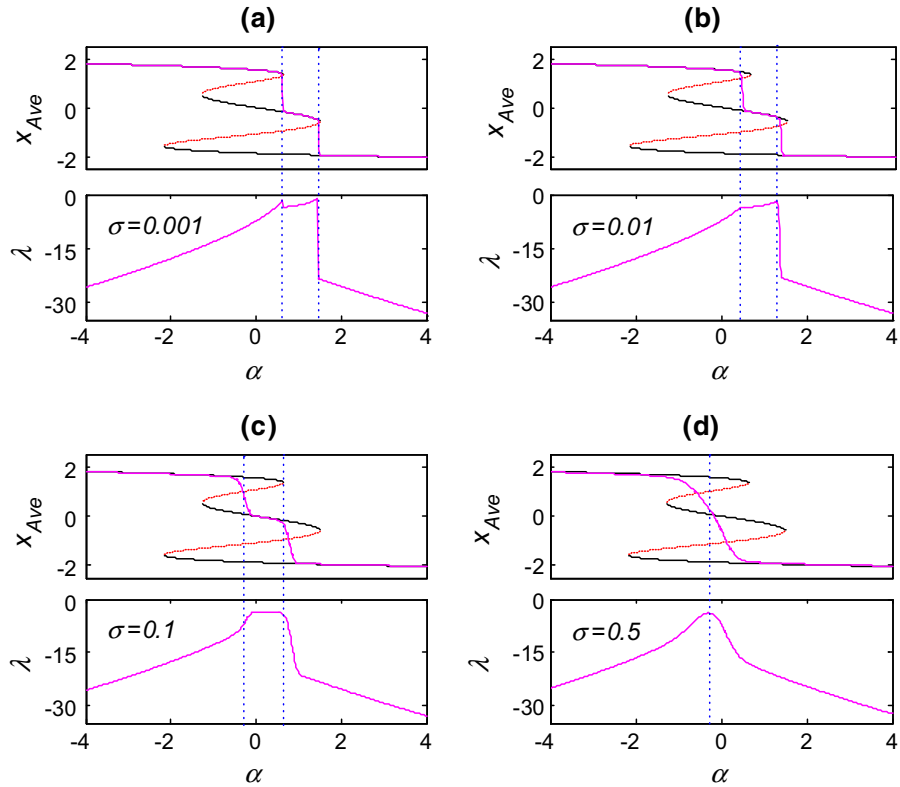

Fig. 4 The λ of system (1) for four different values of σ. The two vertical dashed lines in (**a**–**c**) mark the noise-induced CT1 and CT2. Their forward movements indicate that CT1 and CT2 occur earlier with an increase in σ. A vertical line in (**d**) means that λ cannot clearly identify CT1 and CT2

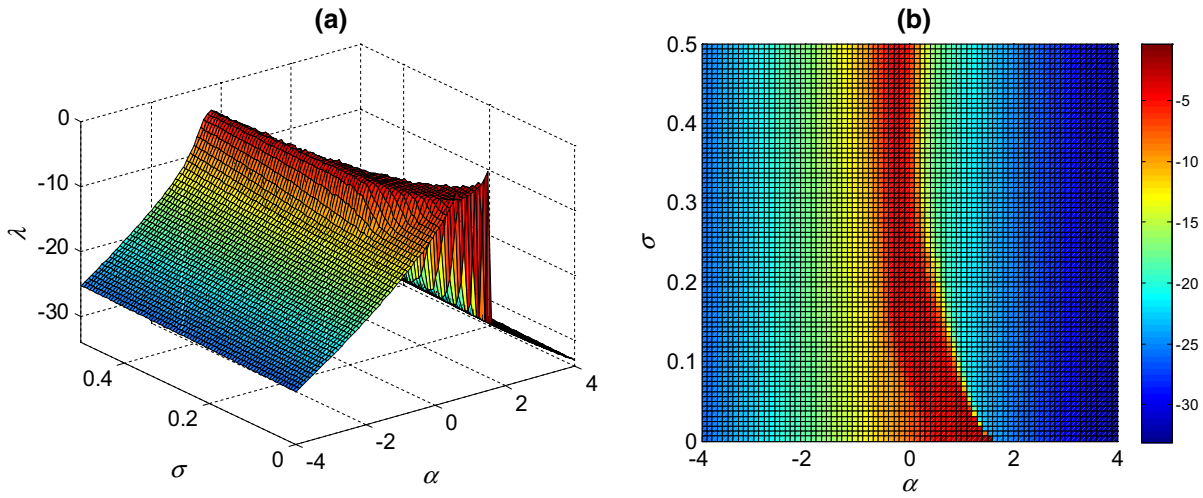

Fig. 5 The 3-D image (**a**) and the corresponding vertical view (**b**) of λ vs α and σ. With σ increasing, λ becomes only one peak shown in (**a**) and it gradually moves to the left shown in (**b**)

4 Shannon entropy

The Shannon entropy, labeled H_s, is another measure to quantify stochastic dynamical characteristics with respect to changing parameters [38, 39]. Here, it is introduced into the prediction of the noise-induced CT1 and CT2 from a new perspective. Let X be a discrete random variable with the possible states $X_1, X_2, \cdots, X_n$, whose corresponding probability is $P_i, i = 1, 2, \cdots, n$. Then, H_s is defined as $H_s = -\sum_{i=1}^{n} P_i \log_2(P_i)$.

Here, H_s will be used as a precursor of the noise-induced critical transitions.

To calculate H_s of system (1), the five parts of α, namely $\alpha < \alpha_{\text{Fold4}}$, $\alpha \in [\alpha_{\text{Fold4}}, \alpha_{\text{Fold2}})$, $\alpha \in [\alpha_{\text{Fold2}}, \alpha_{\text{Fold1}}]$, $\alpha \in (\alpha_{\text{Fold1}}, \alpha_{\text{Fold3}}]$, and $\alpha > \alpha_{\text{Fold3}}$, should be considered, respectively.

For $\alpha < \alpha_{\text{Fold4}}$, the probabilities of system (1) staying in the possible states x_{S1}, x_{S2} and x_{S3} are, respectively, defined as

$$P_{11} = \frac{1}{T}\{t : x(t) > x_{\text{Fold2}}, t \le T\},$$

$$P_{12} = \frac{1}{T}\{t : x_{\text{Fold3}} \le x(t) \le x_{\text{Fold2}}, t \le T\},$$

$$P_{13} = \frac{1}{T}\{t : x(t) < x_{\text{Fold3}}, t \le T\},$$

where T is the time duration of a trajectory. Then, the Shannon entropy in $\alpha < \alpha_{\text{Fold4}}$ can be obtained through

$$H_{s1} = -P_{11}\log_2 P_{11} - P_{12}\log_2 P_{12} - P_{13}\log_2 P_{13}.$$

For $\alpha \in [\alpha_{\text{Fold4}}, \alpha_{\text{Fold2}})$, the expressions of probabilities are

$$P_{21} = \frac{1}{T}\{t : x(t) > x_{\text{Fold2}}, t \le T\},$$

$$P_{22} = \frac{1}{T}\{t : x_{U2} \le x(t) \le x_{\text{Fold2}}, t \le T\},$$

$$P_{23} = \frac{1}{T}\{t : x(t) < x_{U2}, t \le T\},$$

and the corresponding Shannon entropy is

$$H_{s2} = -P_{21}\log_2 P_{21} - P_{22}\log_2 P_{22} - P_{23}\log_2 P_{23}.$$

For $\alpha \in [\alpha_{\text{Fold2}}, \alpha_{\text{Fold1}}]$, the probabilities are

$$P_{31} = \frac{1}{T}\{t : x(t) > x_{U1}, t \le T\},$$

$$P_{32} = \frac{1}{T}\{t : x_{U2} \le x(t) \le x_{U1}, t \le T\},$$

$$P_{33} = \frac{1}{T}\{t : x(t) < x_{U2}, t \le T\},$$

and the corresponding Shannon entropy is

$$H_{s3} = -P_{31}\log_2 P_{31} - P_{32}\log_2 P_{32} - P_{33}\log_2 P_{33}.$$

For $\alpha \in (\alpha_{\text{Fold1}}, \alpha_{\text{Fold3}}]$, the probabilities are

$$P_{41} = \frac{1}{T}\{t : x(t) > x_{\text{Fold2}}, t \le T\},$$

$$P_{42} = \frac{1}{T}\{t : x_{U2} \le x(t) \le x_{\text{Fold2}}, t \le T\},$$

$$P_{43} = \frac{1}{T}\{t : x(t) < x_{U2}, t \le T\},$$

and the corresponding Shannon entropy is

$$H_{s4} = -P_{41}\log_2 P_{41} - P_{42}\log_2 P_{42} - P_{43}\log_2 P_{43}.$$

For $\alpha > \alpha_{\text{Fold3}}$, the probabilities are

$$P_{51} = \frac{1}{T}\{t : x(t) > x_{\text{Fold2}}, t \le T\},$$

$$P_{52} = \frac{1}{T}\{t : x_{\text{Fold3}} \le x(t) \le x_{\text{Fold2}}, t \le T\},$$

$$P_{53} = \frac{1}{T}\{t : x(t) < x_{\text{Fold3}}, t \le T\},$$

and the corresponding Shannon entropy is

$$H_{s5} = -P_{51}\log_2 P_{51} - P_{52}\log_2 P_{52} - P_{53}\log_2 P_{53}.$$

In the simulation on $H_{si}, i = 1, 2, 3, 4, 5$, the initial condition is always set as $x(0) = x_{S1}$ corresponding to different values of α. Furthermore, all $P_{ij}, i = 1, 2, 3, 4, 5$, $j = 1, 2, 3$ are obtained by averaging multiple realizations. Combining these five parts, we get H_s of system (1) as

$$H_s = H_{s1} \cup H_{s2} \cup H_{s3} \cup H_{s4} \cup H_{s5}.$$

Figure 6 shows the H_s of system (1) for different values of σ. It is found that the increase in H_s before the noise-induced CT1 and CT2 appears suddenly when $\sigma = 0.001$. Therefore, there is not enough time to avert them if the critical transition occurs quickly. With σ further increasing, however, an increase in H_s can be easily detected before the impending CT1 or CT2, which indicates that H_s is more efficient to the cases of larger σ. Particularly in Fig. 6d, H_s can still accurately identify CT1 and CT2 even if their intervals become smaller, which is impossible for the largest Lyapunov exponent λ.

In the space diagram of H_s shown in Fig. 7, the ever-present two peaks in H_s indicate its robustness for early warnings of the noise-induced CT1 and CT2. However, two sharp peaks mean that there is not enough time to avert CT1 or CT2, which reflect its limitations on the cases of small σ.

To further validate the robustness of λ and H_s for the identification of multiple noise-induced critical transitions, the comparison of them with the classic parameters, the variance (*Var*) and the autocorrelation at-lag-1 ($R(1)$) [12] at different levels of fluctuations are shown in Fig. 8. Similar to H_s, there is a sudden increase in *Var* before the noise-induced CT1 and CT2 in Fig. 8a. Although an increase always exists in λ and $R(1)$ as the system approaches CT1 or CT2, there is a sudden increase in $R(1)$ when CT2 is imminent, as shown in the enlarged local view. Therefore, there is not enough time to avert CT2 if $R(1)$ is used as the precursor in the case of small fluctuations. However, an increase for λ can be easily detected before the impending CT2. Hence, λ is most suitable as the precursor of critical transitions under small fluctuations. In Fig. 8b, an increase is always present for *Var*, thus, one cannot identify where CT1 or CT2 occurs, while H_s can provide early warning signals for both CT1 and CT2. Therefore, H_s can accurately identify critical transitions under strong fluctuations. However, it needs to be emphasized that there are some challenges to use these two indicators. It requires a long time series or a variety of data to compute λ and H_s [34].

5 Parameter-dependent basin of the unsafe regime

Another precursor criterion proposed here is the parameter-dependent basin of the unsafe regime (PDBUR), i.e., the range of the bifurcation parameter where noise-induced critical transitions may occur. In fact, a noise-induced critical transition occurs when the current stable state is absorbed into another state. For example, the noise-induced CT1 occurs because almost all $x \in [x_{U1}, x_{S1}]$ are absorbed into the sub-desirable state of x_{S2} and CT2 occurs because almost all $x \in [x_{U2}, x_{S2}]$ are absorbed into the undesirable state of x_{S3}. Therefore, the key to judging that a fixed α belongs to PDBUR in the presence of noise is to quantify the absorbed region within the current state. If the proportion of the absorbed region to the current state exceeds a given threshold, it can be argued that system (1) has a great possibility of a critical transition

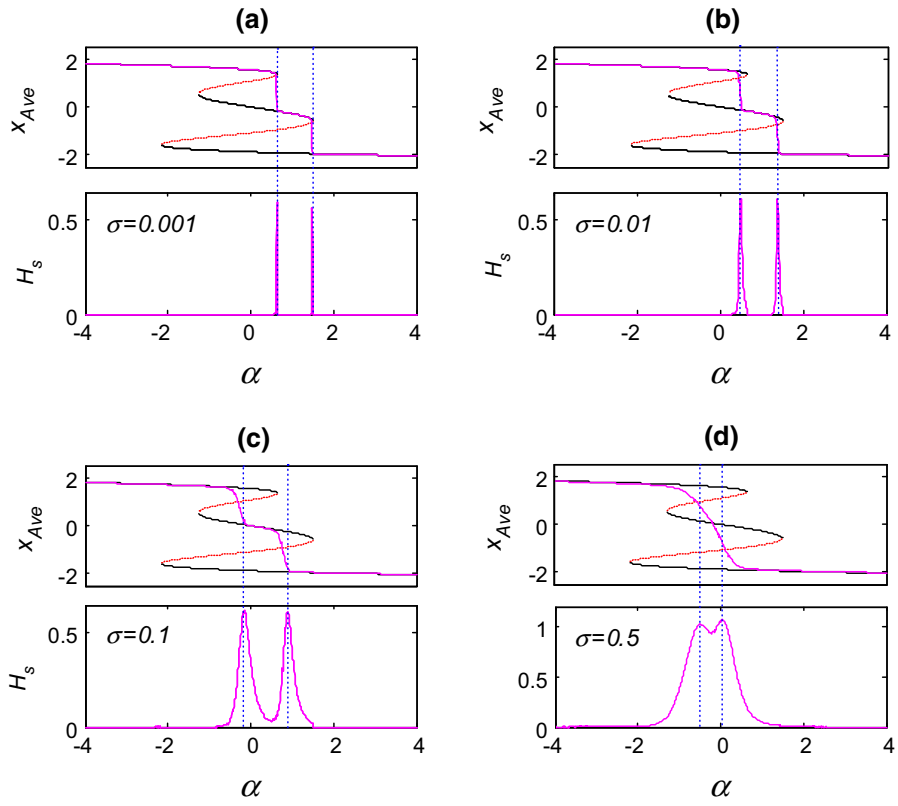

Fig. 6 The H_s of system (1) for four different values of σ. The two vertical dashed lines in (**a**–**d**) mark the noise-induced CT1 and CT2. Their forward movements indicate that CT1 and CT2 occur earlier with an increase in σ

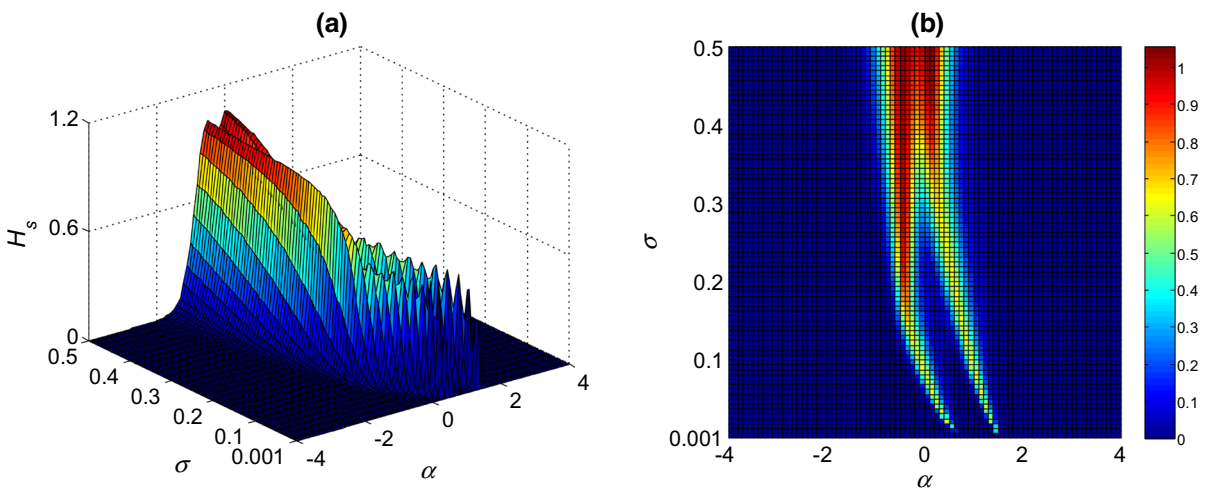

Fig. 7 The 3-D image (**a**) and the corresponding vertical view (**b**) of H_s vs α and σ. There are always two peaks in H_s and they gradually move to the left as shown in (**b**)

and this α belongs to PDBUR. A detailed introduction will be given in the following.

Since a critical transition from the desirable state to the undesirable one is almost impossible for $\alpha \in [\alpha_{\text{Fold4}}, \alpha_{\text{Fold2}})$, only the range of $\alpha \in [\alpha_{\text{Fold2}}, \alpha_{\text{Fold3}}]$, in which the critical transitions may occur under Gaussian white noise, is investigated below.

In the absence of Gaussian white noise, system (1) has three possible states, x_{S1}, x_{S2} and x_{S3}, for

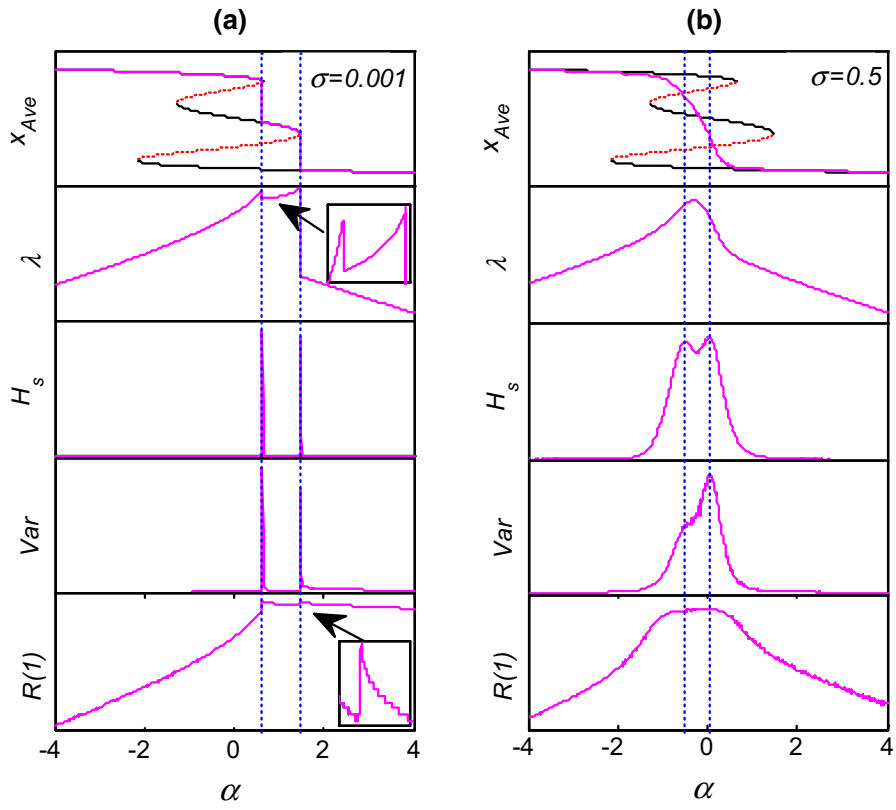

Fig. 8 Comparison between λ, H_s, Var and $R(1)$ for two different σ. The inset plots clearly show the increase before the noise-induced CT2

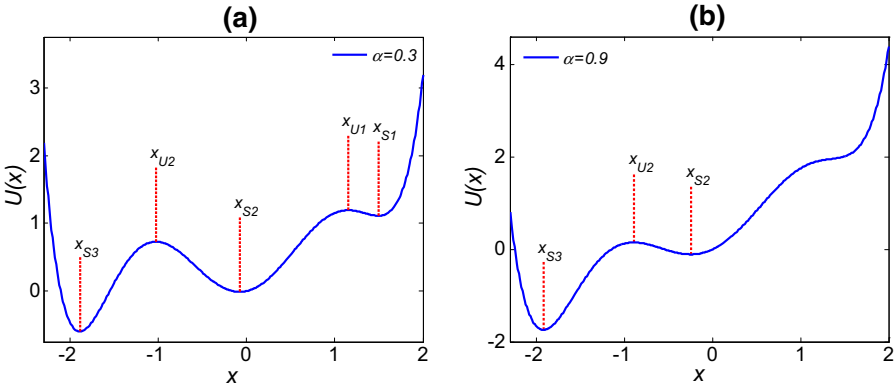

Fig. 9 Potential functions of system (1) with (**a**) $\alpha = 0.3$ that belongs to $[\alpha_{\text{Fold2}}, \alpha_{\text{Fold1}}]$ and (**b**) $\alpha = 0.9$ that belongs to $(\alpha_{\text{Fold1}}, \alpha_{\text{Fold3}}]$

$\alpha \in [\alpha_{\text{Fold2}}, \alpha_{\text{Fold1}}]$, and two possible states, x_{S2} and x_{S3}, for $\alpha \in (\alpha_{\text{Fold1}}, \alpha_{\text{Fold3}}]$. These behaviors can be observed through the potential function $U(x, \alpha)$ with different α shown in Fig. 9.

In Fig. 9a, system (1) starting from a point $x \in [x_{U1}, x_{S1}]$ takes two steps to shift to the undesirable state. The first step is the appearance of CT1 and the second is the occurrence of CT2. Therefore, the absorbed region within $[x_{U1}, x_{S1}]$ and $[x_{U2}, x_{S2}]$ can be calculated, respectively, by taking $[x_{U1}, x_{S1}] \cup [x_{U2}, x_{S2}]$ as the current state of $\alpha = 0.3$. Then, one can determine whether $\alpha = 0.3$ belongs to the range of α where CT1 or CT2 may occur. In Fig. 9b, system (1) shifts to the undesirable state once CT2 takes place. Therefore, $\alpha = 0.9$ can be determined whether it belongs to the range of α where CT2 may occur via counting the absorbed region within $[x_{U2}, x_{S2}]$. In

Table 1 The current states of system (1) for two different values of α

α	Current states
0.3	$[x_{U1}, x_{S1}] \cup [x_{U2}, x_{S2}] = [1.152, 1.494] \cup [-1.028, -0.079]$
0.9	$[x_{U2}, x_{S2}] = [-0.895, -0.247]$

Table 1, the current states of system (1) corresponding to these two different α are presented.

In fact, the noise-induced CT1 occurs because most of $x \in [x_{U1}, x_{S1}]$ exiting from the left side x_{U1}, and CT2 occurs because $x \in [x_{U2}, x_{S2}]$ exiting from the left side x_{U2}. Therefore, one can quantify the absorbed region within $[x_{U1}, x_{S1}]$ or $[x_{U2}, x_{S2}]$ via analyzing the escape probability $P_1(x)$ of $x \in [x_{U1}, x_{S1}]$ or $P_2(x)$ of $x \in [x_{U2}, x_{S2}]$. They can be described through

$$\mathcal{L}P_i(x) = f(x, \alpha)\frac{dP_i(x)}{dx} + \frac{\sigma}{2}\frac{d^2P_i(x)}{dx^2} = 0 \quad i = 1, 2, \tag{5}$$

where $\mathcal{L}$ is a generator [40]. The boundary conditions of Eq. (5) are set as $P_1(x)|_{x=x_{U1}} = 1, P_1(x)|_{x=x_{S1}} = 0$ for $x \in [x_{U1}, x_{S1}]$, and $P_2(x)|_{x=x_{U2}} = 1$, $P_2(x)|_{x=x_{S2}} = 0$ for $x \in [x_{U2}, x_{S2}]$.

From Fig. 2, we observe that CT1 occurs at $\alpha = 0.3$ for $\sigma = 0.1$ and $\sigma = 0.5$. To obtain some generic behavior of $P_1(x)$ when noise-induced CT1 occurs, the $P_1(x)$ values of these two special cases are calculated as shown in Fig. 10. It is found that $P_1(x)$ is very close to $y_1(x)$ when $\sigma = 0.5$, which means that the tangent

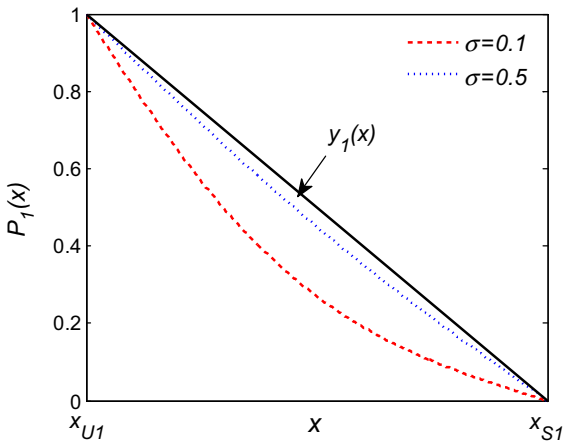

Fig. 10 The $P_1(x)$ of $x \in [x_{U1}, x_{S1}]$ for $\alpha = 0.3$ and two different values of σ. $y_1(x) = \frac{1}{x_{U1}-x_{S1}}x + \frac{x_{S1}}{x_{S1}-x_{U1}}$ is a line connecting $(x_{U1}, 1)$ and $(x_{S1}, 0)$ in x-$P_1(x)$ plane

slope of $P_1(x)$ is very close to $\frac{1}{x_{U1}-x_{S1}}$ if $[x_{U1}, x_{S1}]$ is almost absorbed. Therefore, we can quantify an absorbed region by analyzing the relationship between the tangent slope of $P_1(x)$ and the slope of $y_1(x)$. Here, we approximately take $\frac{1}{2} \times \frac{1}{x_{U1}-x_{S1}}$ as a critical value of the tangent slope of $P_1(x)$ to define the absorbed region within $[x_{U1}, x_{S1}]$. In fact, this interesting phenomenon is also true for the noise-induced CT2. Because the line in x-$P_2(x)$ plane is $y_2(x) = \frac{1}{x_{U2}-x_{S2}}x + \frac{x_{S2}}{x_{S2}-x_{U2}}$ that connects $(x_{U2}, 1)$ and $(x_{S2}, 0)$, the critical value is taken as $\frac{1}{2} \times \frac{1}{x_{U2}-x_{S2}}$ to define the absorbed region within $[x_{U2}, x_{S2}]$. In the following, the absorbed region within $[x_{U1}, x_{S1}]$ or $[x_{U2}, x_{S2}]$ is defined.

Definition 1 For $\alpha \in [\alpha_{\text{Fold2}}, \alpha_{\text{Fold1}}]$, suppose that two finite sequences $x_{U1} = x_0 < x_1 < \cdots < x_{M-1} < x_M = x_{S1}$ and $x_{U2} = x_0 < x_1 < \cdots < x_{N-1} < x_N = x_{S2}$ are tagged partitions of $[x_{U1}, x_{S1}]$ and $[x_{U2}, x_{S2}]$, respectively. The set

$$[x_{U1}, x_{M-k}] \cup [x_{U2}, x_{N-j}]$$

satisfying $\frac{P_1(x_{M-k-1})-P_1(x_{M-k})}{x_{M-k-1}-x_{M-k}} \le \frac{1}{2(x_{U1}-x_{S1})}$ and $\frac{P_2(x_{N-j-1})-P_2(x_{N-j})}{x_{N-j-1}-x_{N-j}} \le \frac{1}{2(x_{U2}-x_{S2})}$ is defined as the absorbed region of $[x_{U1}, x_{S1}] \cup [x_{U2}, x_{S2}]$ under σ. Here, $x_{U1} < x_{n-k} \le x_{S1}, k = 0, 1, \cdots, m-1, x_{U2} < x_{n-j} \le x_{S2}, j = 0, 1, \cdots, n-1$, and $[x_{U1}, x_{M-k}]$ is denoted as D_1, $[x_{U2}, x_{N-j}]$ is denoted as D_2.

Definition 2 For $\alpha \in (\alpha_{\text{Fold1}}, \alpha_{\text{Fold3}}]$, suppose that a tagged partition of $[x_{U2}, x_{S2}]$ is a finite sequence

$$x_{U2} = x_0 < x_1 < \cdots < x_{L-1} < x_L = x_{S2}.$$

The set

$$[x_{U2}, x_{L-l}], x_{U2} < x_{L-l} \le x_{S2}, l = 0, 1, \ldots, L-1$$

satisfying $\frac{P_2(x_{L-l-1})-P_2(x_{L-l})}{x_{L-l-1}-x_{N-l}} \le \frac{1}{2(x_{U2}-x_{S2})}$ is defined as the absorbed region of $[x_{U2}, x_{S2}]$ under σ, and $[x_{U2}, x_{L-l}]$ is denoted as D_3.

Based on Definitions 1 and 2, the escape probability and the corresponding absorbed region for different values of α and σ are shown in Fig. 11. In addition, the interval durations of $D_1 \cup D_2$ and D_3 are presented in Table 2. It is found that D_1, D_2 and D_3 increase with increasing σ. When $\sigma = 0.5$, even the entire $[x_{U1}, x_{S1}]$ becomes D_1 as shown in Fig. 11a, and the whole $[x_{U2}, x_{S2}]$ becomes D_3 as shown in Fig. 11b, which indicate that the corresponding CT1 and CT2 must

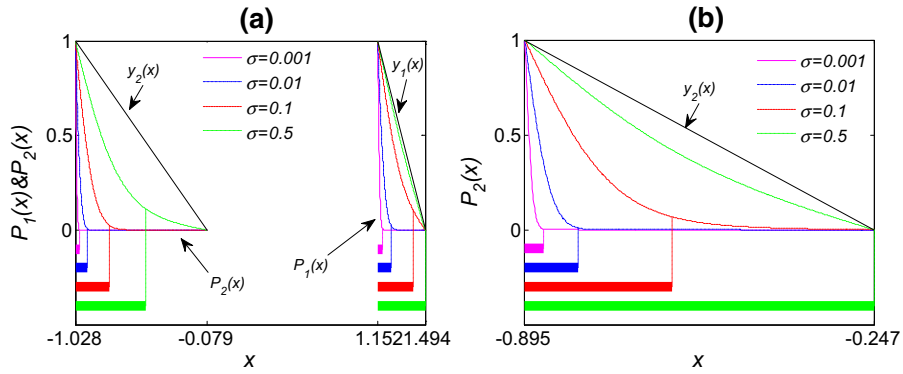

Fig. 11 The escape probability and the corresponding absorbed region (bar-type) for different values of σ. **a** $\alpha = 0.3$ with $[x_{U2}, x_{S2}] \cup [x_{U1}, x_{S1}] = [-1.028, -0.079] \cup [1.152, 1.494]$. **b** $\alpha = 0.9$ with $[x_{U2}, x_{S2}] = [-0.895, -0.247]$

Table 2 The interval durations of $D_1 \cup D_2$ and D_3 for different values of α and σ

α	σ			
	0.001	0.01	0.1	0.5
0.3	[1.152,1.187]∪[− 1.028, − 0.996]	[1.152,1.247]∪[− 1.028, − 0.939]	[1.152,1.407]∪[− 1.028, − 0.780]	[1.152,1.494]∪[− 1.028, − 0.519]
0.9	[− 0.895, − 0.861]	[− 0.895, − 0.797]	[− 0.895, − 0.621]	[− 0.895, − 0.247]

occur. Although CT2 occurs for $\alpha = 0.9$ and $\sigma = 0.1$ as shown in Fig. 2, $[x_{U2}, x_{S2}]$ does not completely become D_3 in this case.

Supposing μ is a measurement of the interval duration, the natural questions are: For $\alpha \in [\alpha_{\text{Fold2}}, \alpha_{\text{Fold1}}]$, how large is $\frac{\mu(D_1)}{\mu([x_{U1}, x_{S1}])} \triangleq \mu_1$ or $\frac{\mu(D_2)}{\mu([x_{U2}, x_{S2}])} \triangleq \mu_2$ for the corresponding CT1 or CT2 to occur? For $\alpha \in (\alpha_{\text{Fold1}}, \alpha_{\text{Fold3}}]$, how large is $\frac{\mu(D_3)}{\mu([x_{U2}, x_{S2}])} \triangleq \mu_3$ for the corresponding CT2 to occur? These questions will be answered below.

Reconsidering the noise-induced CT1 and CT2 with $\sigma = 0.001$ as shown in Fig. 12, it is found that system (1) is about to leave the desirable state when $\alpha = 0.61$ and leave it when $\alpha = 0.62$ for the case of CT1. Furthermore, system (1) is about to leave the sub-desirable state when $\alpha = 1.47$ and leave it when $\alpha = 1.48$ for the case of CT2. Since

$$\left.\frac{\mu(D_1)}{\mu([x_{U1}, x_{S1}])}\right|_{\alpha=0.61} = 0.363 \triangleq \mu_{\alpha=0.61},$$

and

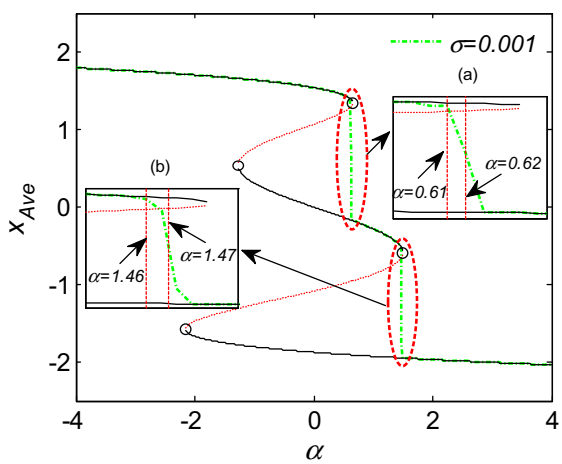

Fig. 12 Noise-induced CT1 and CT2 in system (1) for $\sigma = 0.001$. The inset plots (a) and (b) are enlarged local views

$$\left.\frac{\mu(D_1)}{\mu([x_{U1}, x_{S1}])}\right|_{\alpha=0.62} = 0.414 \triangleq \mu_{\alpha=0.62},$$

one may approximately take the critical value about CT1 in $\alpha \in [\alpha_{\text{Fold2}}, \alpha_{\text{Fold1}}]$ as

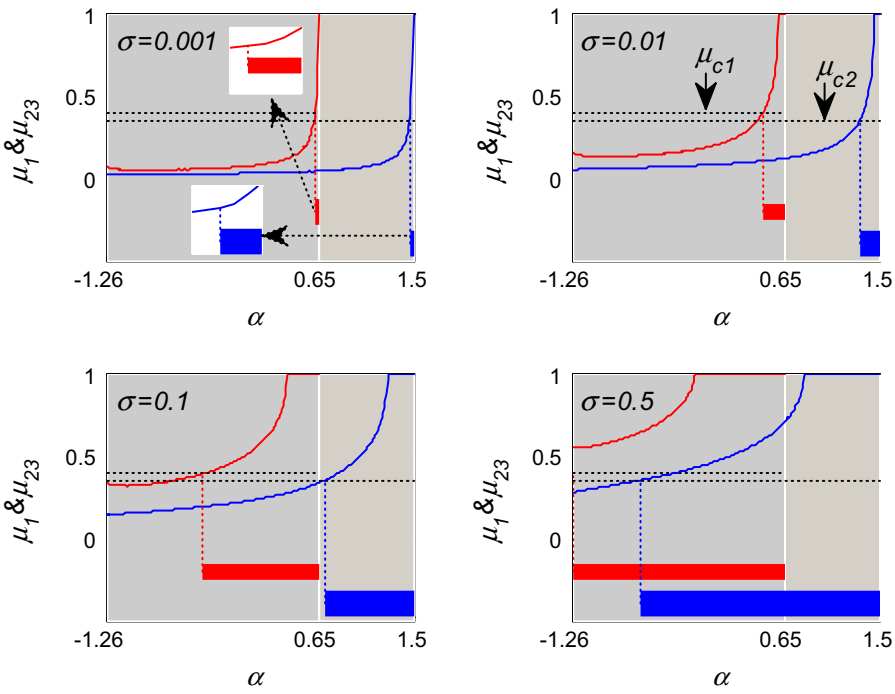

Fig. 13 The μ_1 (top solid line) and $(\mu_2 \cup \mu_3) \triangleq \mu_{23}$ (bottom solid line), and the corresponding U_{CT1} (thin bar-type) and U_{CT2} (thick bar-type) of α under four different values of σ. The two dotted lines are μ_{c1} and μ_{c2}, respectively

$$\frac{1}{2}(\mu_{\alpha=0.61} + \mu_{\alpha=0.62}) = 0.389 \triangleq \mu_{c1}.$$

Similarly, the critical value about CT2 in $\alpha \in (\alpha_{\mathrm{Fold1}}, \alpha_{\mathrm{Fold3}}]$ is taken as

$$\frac{1}{2}\left(\frac{\mu(D_3)}{\mu([x_{U2}, x_{S2}])}\bigg|_{\alpha=1.47} + \frac{\mu(D_3)}{\mu([x_{U2}, x_{S2}])}\bigg|_{\alpha=1.48}\right) = \frac{1}{2}(\mu_{\alpha=1.47} + \mu_{\alpha=1.48}) = 0.348 \triangleq \mu_{c2}.$$

The μ_{c2} is also the critical value about CT2 in $\alpha \in [\alpha_{\mathrm{Fold2}}, \alpha_{\mathrm{Fold1}}]$.

Then, the regions of α and σ where noise-induced CT1 or CT2 may occur will be quantified in the following.

Definition 3 Suppose that $D_1 \cup D_2$ is the absorbed region within $[x_{U1}, x_{S1}] \cup [x_{U2}, x_{S2}]$. The set of α that satisfies

$$\mu_1 = \frac{\mu(D_1)}{\mu([x_{U1}, x_{S1}])} \geq \mu_{c1} \text{ or } \mu_2 = \frac{\mu(D_2)}{\mu([x_{U2}, x_{S2}])} \geq \mu_{c2}$$

is defined as the PDBUR of noise-induced CT1 or CT2 in $\alpha \in [\alpha_{\mathrm{Fold2}}, \alpha_{\mathrm{Fold1}}]$, which is denoted as $U_1(\alpha, \sigma) \cup U_2(\alpha, \sigma)$.

Definition 4 Suppose that D_3 is the absorbed region within $[x_{U2}, x_{S2}]$. The set of α satisfying

$$\mu_3 = \frac{\mu(D_3)}{\mu([x_{U2}, x_{S2}])} \geq \mu_{c2}$$

is defined as the PDBUR of noise-induced CT2 in $\alpha \in (\alpha_{\mathrm{Fold1}}, \alpha_{\mathrm{Fold3}}]$, which is denoted as $U_3(\alpha, \sigma)$.

According to these two definitions, one can see that the PDBUR of Gaussian white noise-induced CT1 is $U_1(\alpha, \sigma) \triangleq U_{\mathrm{CT1}}$, and the PDBUR of CT2 is $U_2(\alpha, \sigma) \cup U_3(\alpha, \sigma) \triangleq U_{\mathrm{CT2}}$.

Based on Definitions 3 and 4, the μ_1, μ_{23}, and the corresponding U_{CT1}, U_{CT2} for four different values of σ are shown in Fig. 13. The results show that U_{CT1} and U_{CT2} increase with the increase in σ. In the case of $\sigma = 0.5$, even the entire $\alpha \in [\alpha_{\mathrm{Fold2}}, \alpha_{\mathrm{Fold1}}]$ becomes U_{CT1} and the whole $\alpha \in (\alpha_{\mathrm{Fold1}}, \alpha_{\mathrm{Fold3}}]$ becomes $U_3(\alpha, \sigma)$. Moreover, it can be found that CT2 occurs after CT1 occurring through the change of $U_2(\alpha, \sigma)$ in $\alpha \in [\alpha_{\mathrm{Fold2}}, \alpha_{\mathrm{Fold1}}]$. This is because system (1) staying in the desirable state will first switch to the sub-desirable state and then shift to the undesirable state under Gaussian white noise.

Figure 14 shows the space diagrams about U_{CT1} and U_{CT2}. Once α and σ belong to U_{CT1} or U_{CT2}, there

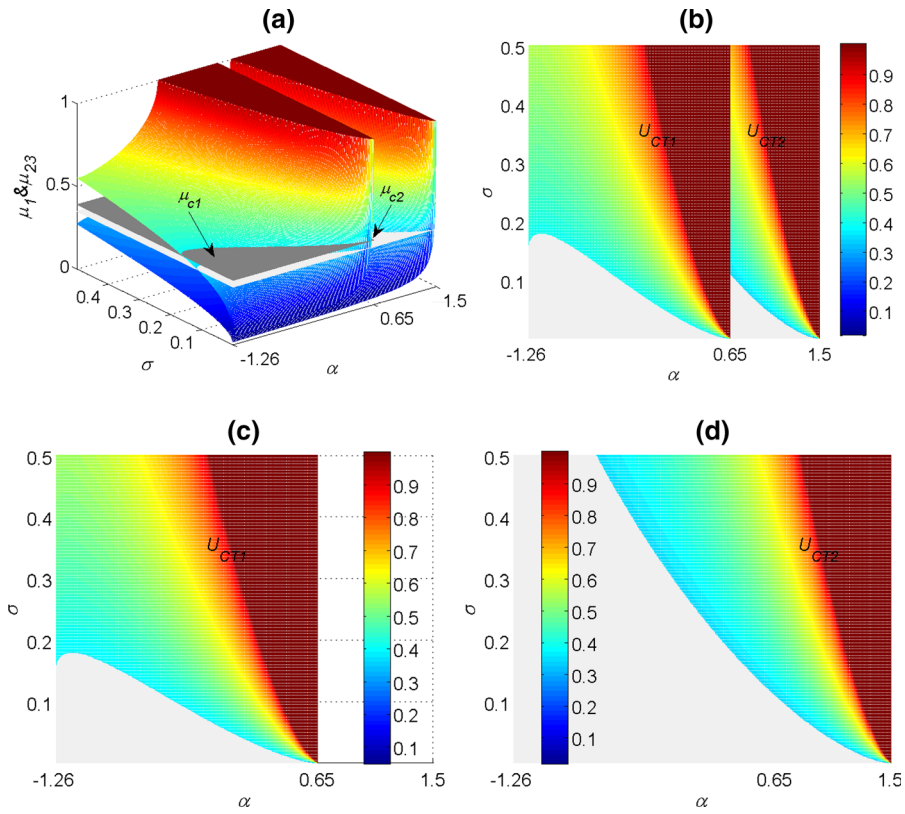

Fig. 14 The space diagrams about U_{CT1} and U_{CT2}. **a** The μ_1 (upper curved surface) and μ_{23} (lower curved surface) about α and σ. Two inserted planes represent μ_{c1} and μ_{c2}, respectively. **b** The U_{CT1} and U_{CT2}. **c** The U_{CT1} of CT1. **d** The U_{CT2} of CT2

is a high possibility that CT1 or CT2 is impending. As shown in Fig. 14b, there is an intersection between U_{CT1} and U_{CT2} in $\alpha \in [\alpha_{\mathrm{Fold2}}, \alpha_{\mathrm{Fold1}}]$. It does not mean that CT1 and CT2 occur at the same time. However, it only shows that, in this intersection, CT2 is very likely to occur after CT occurring. Although the occurrence of CT1 may have less impact on the operation of some practical systems, it is needed to avoid α and σ from entering U_{CT1}, as shown in Fig. 14c. Once α and σ enter U_{CT1}, the possibility of CT2 occurring increases. However, the occurrence of CT2 often causes catastrophic damage. Therefore, one needs to take some measures to avoid the emergence of U_{CT2}.

6 Conclusions

In this paper, three precursor criteria for Gaussian white noise-induced critical transitions between multi-stable states are investigated via taking a tri-stable model for a case study. By introducing the largest Lyapunov exponent and the Shannon entropy into the prediction of the noise-induced multiple critical transitions, it is found that the largest Lyapunov exponent can be acted as an efficient precursor criterion in the case of small fluctuations, while the Shannon entropy can accurately identify critical transitions under strong fluctuations. Compared with the classic variance and autocorrelation at-lag-1, both of them are more efficient. In addition, the definitions of the PDBUR are given. Based on these definitions, we can approximately quantify the range of the bifurcation parameter, where the noise-induced CT1 or CT2 may occur. Although these precursor criteria can provide some options for predicting the multiple noise-induced critical transitions in multi-stable models, their applicability to more general practical systems needs to be further explored.

Acknowledgments This study was supported by the National Natural Science Foundation of China under Grant No. 11772255, the Fundamental Research Funds for the Central Universities, the Shaanxi Project for Distinguished Young

Scholars, the Research Funds for Interdisciplinary Subject of Northwestern Polytechnical University and Shaanxi Provincial Key R&D Program 2020KW-013 and 2019TD-010. Y. Li thanks the China Postdoctoral Science Foundation funded project.

Compliance with ethical standards

Conflict of interest No conflict of interest exists in the submission of this manuscript, and manuscript is approved by all authors for publication. This work was original research, has not been published previously, and not under consideration for publication elsewhere in whole or in part.

References

1. Feudel, U.: Complex dynamics in multistable systems. Int. J. Bifurcat. Chaos **18**(06), 1607–1626 (2008)
2. Feudel, U., Pisarchik, A.N., Showalter, K.: Multistability and tipping: from mathematics and physics to climate and brain-Minireview and preface to the focus issue. Chaos **28**(3), 033501 (2018)
3. Knorre, W., Bergter, F., Simon, Z.: Multistability in metabolic systems. Stud. Biophys. **49**, 81–89 (1975)
4. Li, Y.G., Xu, Y., Kurths, J., Yue, X.L.: Lévy-noise-induced transport in a rough triple-well potential. Phys. Rev. E **94**(4), 042222 (2016)
5. Marmillot, P., Kaufman, M., Hervagault, J.F.: Multiple steady states and dissipative structures in a circular and linear array of three cells: numerical and experimental approaches. J. Chem. Phys. **95**(2), 1206–1214 (1991)
6. Yuan, R.S., Zhu, X.M., Wang, G.W., Li, S.T., Ao, P.: Cancer as robust intrinsic state shaped by evolution: a key issues review. Rep. Prog. Phys. **80**(4), 042701 (2017)
7. Power, S.B., Kleeman, R.: Multiple equilibria in a global ocean general circulation model. J. Phys. Oceanogr. **23**(8), 1670–1681 (1993)
8. Ditlevsen, P.D., Johnsen, S.J.: Tipping points: early warning and wishful thinking. Geophys. Res. Lett. **37**(37), L19703 (2010)
9. Barnosky, A.D., et al.: Approaching a state shift in earth's biosphere. Nature **486**(7401), 52–58 (2012)
10. Stolbova, V., Surovyatkina, E., Bookhagen, B., Kurths, J.: Tipping elements of the Indian monsoon: prediction of onset and withdrawal. Reophys. Res. Lett. **43**(8), 3982–3990 (2016)
11. Ma, J.Z., Xu, Y., Xu, W., Li, Y.G., Kurths, J.: Slowing down critical transitions via Gaussian white noise and periodic force. Sci. China Technol. Sc. **62**(12), 2144–2152 (2019)
12. Dakos, V., et al.: Methods for detecting early warnings of critical transitions in time series illustrated using simulated ecological data. PLoS ONE **7**(7), e41010 (2012)
13. Scheffer, M., et al.: Early-warning signals for critical transitions. Nature **461**(7260), 53–59 (2009)
14. Carpenter, S.R., Brock, W.A.: Rising variance: a leading indicator of ecological transition. Ecol. Lett. **9**(3), 311–318 (2006)
15. Dakos, V., et al.: Slowing down as an early warning signal for abrupt climate change. PNAS **105**(38), 14308–14312 (2008)
16. Wissel, C.: A universal law of the characteristic return time near thresholds. Oecologia **65**(1), 101–107 (1984)
17. Guttal, V., Jayaprakash. C.: Changing skewness: an early warning signal of regime shifts in ecosystems. Ecol. Lett. **11**(5), 450-460 (2008)
18. Brock, W.A., Carpenter, S.R.: Interacting regime shifts in ecosystems: implication for early warnings. Ecol. Monogr. **80**(3), 353–367 (2010)
19. Dakos, V., van Nes, E.H., Donangelo, R., Fort, H., Scheffer, M.: Spatial correlation as leading indicator of catastrophic shifts. Theor. Ecol. **3**(3), 163–174 (2010)
20. Scheffer, M., Carpenter, S., Foley, J.A., Folke, C., Walker, B.: Catastrophic shifts in ecosystems. Nature **413**(6856), 591–596 (2001)
21. Moreau, L., Sontag, E.: Balancing at the border of instability. Phys. Rev. E **68**(2), 020901 (2003)
22. Kuehn, C.: A mathematical framework for critical transitions: bifurcations, fast-slow systems and stochastic dynamics. Physica D **240**(12), 1020–1035 (2011)
23. Ma, J.Z., Xu, Y., Kurths, J., Wang, H.Y., Xu, W.: Detecting early-warning signals in periodically forced systems with noise. Chaos **28**(11), 113601 (2018)
24. Hramov, A.E., Koronovskii, A.A., Kurovskaya, M.K.: Zero Lyapunov exponent in the vicinity of the saddle-node bifurcation point in the presence of noise. Phys. Rev. E **78**(3), 036212 (2008)
25. Farazmand, M., Sapsis, T.P.: Dynamical indicators for the prediction of bursting phenomena in high-dimensional systems. Phys. Rev. E **94**(3), 032212 (2016)
26. Nazarimehr, F., Rajagopal, K., Khalaf, A.J.M., Alsaedi, A., Pham, V.T., Hayat, T.: Investigation of dynamical properties in a chaotic flow with one unstable equilibrium: circuit design and entropy analysis. Chaos, Solitons Fractals **115**, 7–13 (2018)
27. Menck, P.J., Heitzig, J., Marwan, N., Kurths, J.: How basin stability complements the linear-stability paradigm. Nat. Phys. **9**(2), 89–92 (2013)
28. Serdukova, L., Zheng, Y.Y., Duan, J.Q., Kurths, J.: Stochastic basins of attraction for metastable states. Chaos **26**(7), 073117 (2016)
29. Ma, J.Z., Xu, Y., Li, Y.G., Tian, R.L., Kurths, J.: Predicting noise-induced critical transitions in bistable systems. Chaos **29**(8), 081102 (2019)
30. Ao, P., Galas, D., Hood, L., Zhu, X.M.: Cancer as robust intrinsic state of endogenous molecular-cellular network shaped by evolution. Med. Hypotheses **70**(3), 678–684 (2008)
31. Wang, Z.Q., Xu, Y., Yang, H.: Lévy noise induced stochastic resonance in an FHN model. Sci. China Technol. Sc. **59**(3), 371–375 (2016)
32. Xu, Y., Zan, W.R., Jia, W.T., Kurths, J.: Path integral solutions of the governing equation of SDEs excited by Lévy white noise. J. Comp. Phys. **394**(1), 41–55 (2019)
33. Gardiner, C.W., et al.: Handbook of Stochastic Methods. Springer, Berlin (1985)
34. Nazarimehr, F., Jafari, S., Golpayegani, S.M.R.H., Sprott, J.C.: Can Lyapunov exponent predict critical transitions in

biological systems? Nonlinear Dyn. **88**(2), 1493–1500 (2017)
35. Nazarimehr, F., Jafari, S., Golpayegani, S.M.R.H., Perc, M., Sprott, J.C.: Predicting tipping points of dynamical systems during a period-doubling route to chaos. Chaos **28**(7), 073102 (2018)
36. Benettin, G., Galgani, L., Giorgilli, A., Strelcyn, J.M.: Lyapunov exponents for smooth dynamical systems and Hamiltonian systems; a method for computing all of them, Part I: Theory. Meccanica **15**, 9–20 (1980)
37. Benettin, G., Galgani, L., Giorgilli, A., Strelcyn, J.M.: Lyapunov exponents for smooth dynamical systems and Hamiltonian systems; a method for computing all of them, Part II: numerical application. Meccanica **15**, 21–30 (1980)
38. Venkatramani, J., Sarkar, S., Gupta, S.: Investigations on precursor measures for aeroelastic flutter. J. Sound Vib. **419**, 318–336 (2018)
39. Wu, J., Xu, Y., Wang, H.Y., Kurths, J.: Information-based measures for logical stochastic resonance in a synthetic gene network under Lévy flight superdiffusion. Chaos **27**(6), 063105 (2017)
40. Gao, T., Duan, J.Q., Li, X.F., Song, R.M.: Mean exit time and escape probability for dynamical systems driven by Lévy noises. SIAM J. Sci. Comput. **36**(3), A887–A906 (2014)